JOURNAL OF MATERIALS SCIENCE 32 (1997) 2707–2714

The influence of the elastic modulus on computed craze surface stress distributions

L. BEVAN*, L. KÖNCZÖL, W. DÖLL
Fraunhofer-Institut für Werkstoffmechanik, Wöhlerstrasse 11, D-79108 Freiburg, Germany

The surface stresses along the contour of a crack-tip craze in a glassy thermoplastic can be computed from measured craze displacements by applying finite element methods. It is shown that calculated crack-tip craze surface stress distributions are highly dependent on the accuracy of the evaluation of the elastic modulus of the bulk polymer. Methods of estimating the modulus are considered. A method based on fitting the Dugdale model to the measured craze profile gives rate- and time-dependent moduli which are consistent with measured moduli at strain levels comparable with those in the compact tension specimen near the interface with the craze. The major part of the sample is at a much lower strain level and a new method, based on interference optical measurements and finite element computations of crack displacements, is developed to estimate the appropriate modulus. Craze surface stresses are computed for two cases in which the estimated modulus for the two parts of the sample significantly differ. In a creep test, the modulus near the craze is lower than that in the remainder of the specimen and it is seen that any stress concentration at the crack tip is suppressed. This explains why the crack remains stationary while the craze continues to grow. In the case of crack propagation, the modulus in the region around the craze has the higher value and the stress at the crack tip increases. The crack therefore continues to propagate.

1. Introduction

The finite element method has been previously used to compute, from interference optics measurements, surface stress distributions for crack-tip crazes under static [1], quasi-static [2] and fatigue [3] loading. The stress distributions may differ in detail but, nevertheless, there is a general similarity with a maximum at the crack tip followed by a sharp decrease and then either an almost constant stress or a very gradual stress decrease over most of the craze length. Close to the craze tip another stress peak may arise, depending on craze tip profile as measured or extrapolated starting from the last interference fringe, respectively. In the computation of stresses a constant modulus in the compact tension specimen is assumed. Its value was obtained from the measured craze profile, using the method described in section 3.2.1. On different time stages it was in good agreement with measured [4] time-dependent moduli at a strain level similar to that in the polymer in the close vicinity of the craze. However, the strain is low in the major part of the specimen, and the modulus will differ from that in the region near the craze. Thus the question arises as to whether or not this may influence the craze stress distribution. Therefore initially a new method, is developed to estimate the bulk modulus based on crack displacements. Second, craze surface stress distributions, based on the two moduli, are computed and are compared with those obtained by the previous method.

2. Experimental and computational procedures

2.1. Experimentation

The geometry of single crack tip crazes as well as crack openings in transparent thermoplastics can be measured using optical interferometry [4]. The crack tip area with a craze in a fracture mechanics specimen (e.g. compact tension (CT) type, as shown in Fig. 1) is illuminated in reflection with monochromatic light, yielding interference fringe patterns. In order to calculate the crack openings and craze thicknesses, the positions of the individual fringes relative to the crack tip are determined by scanning in a microdensitometer. The thickness $2v$ of crack and craze opening at position x are given by basic interference theory by

$$2v(x) = \frac{\lambda}{2\mu}(n - 1/2) \tag{1}$$

where n is the fringe order ($n = 1, 2, 3 \ldots$ at bright fringes and $n = 1.5, 2.5, 3.5 \ldots$ at dark fringes), λ is the wavelength of the light and μ is the refractive index within a crack or craze.

* Present address: Universität Erlangen-Nürnberg, Lehrstuhl für Kunststofftechnik, Am Weichselgarten 9, D-91058 Erlangen-Tennenlohe, Germany

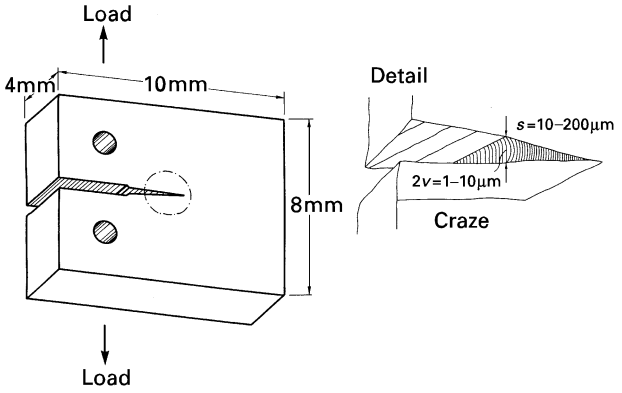

Figure 1 Sketch of a compact tension (CT) specimen as used for interferometric measurement of craze contours with detail enlargement of the crack tip area with a craze zone.

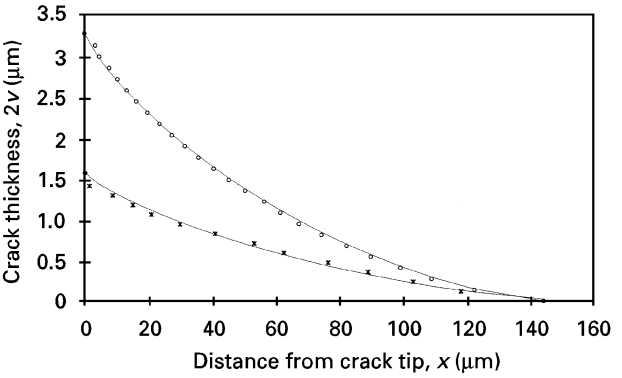

Figure 2 Evaluated openings (with Dugdale fit of the craze contour) of a crack tip craze in PMMA as measured interferometrically in the (○) loaded ($K_I = 0.54$ MPa $m^{1/2}$) and the (*) unloaded state.

To determine the strain dependent refractive index μ_c of the crazed material the stretch on the polymeric matter within the craze has to be quantified. This is performed according to the following procedure [3]:

The craze extension ratio Λ_c is defined by

$$\Lambda_c = \frac{2v}{\tau_o} \tag{2}$$

where τ_o is the primordial thickness, that is the thickness of the layer of bulk which fibrillates to form a craze. The craze extension ratio may also be obtained from the following equation, coupling the Lorentz–Lorenz equation with interference optics theory

$$\frac{\mu_c^2 - 1}{\mu_c^2 + 2} = \frac{\mu_b^2 - 1}{\mu_b^2 + 2}\frac{1}{\Lambda_c} \tag{3}$$

where μ_b is the refractive index of the bulk polymer.

Since the value μ_c of the refractive index of the craze in the unloaded state is known from independent measurements [4], as is μ_b, the primordial thickness profile can be readily obtained from the interference optics measurements on the unloaded craze.

The refractive index of the loaded craze can be estimated from the ratio of the fringe numbers in the loaded and the unloaded craze, i.e., n_1/n_0. This index is used as a first estimate of μ_c and the craze thickness is obtained at various positions corresponding to the distances of the interference fringes from the crack tip. The values of Λ_c given by Equations 2 and 3 are compared and an iterative approach is used, adjusting the estimate of μ_c, if necessary, until consistent results are obtained.

The symbols (*) for the loaded and (o) for the unloaded craze in Fig. 2 exhibit the data of the fringe patterns taken from a craze in poly(methyl melarate) (PMMA), in the loaded and the unloaded states as evaluated with Equation 1 using refractive indices determined according to the procedure described above.

The position of the craze tip and the maximum craze width, $2v$, at the very crack tip, indicated in Fig. 2 by the symbols (●), have to be estimated by extrapolation of the measured data. This can be performed using fracture mechanics models, such as the Dugdale model as described in Section 3.2.1, or by fitting mathematical curves of different orders. In the case of PMMA as shown in Fig. 2 the Dugdale fit gives reasonable results.

In the evaluation of the crack opening using Equation 1 the refractive index of air, $\mu = 1$, has to be used. However, in contrast to the interference fringe pattern of the craze zone, the fringes of the crack opening do not begin with fringe order $n = 1$ but with a larger number due to the crack tip displacement. If the fringe order at the crack tip is not determined by counting the fringes passing the crack tip during specimen loading, then it has to be estimated later by other means. As a first estimate the fringe order in the craze next to the crack tip may be used, followed by further adjustments as described in Section 3.2.3.

2.2. Finite element analysis

The finite element code currently used is ADINA [5] with a mesh that differs from that used previously. The mesh has been redesigned while retaining the general approach of a fine mesh in the craze and crack tip region, with a transition to a coarser mesh in the bulk of the compact tension specimen. The region from the crack edge to the loading pins is ignored and, in the fine mesh, the number of elements is reduced without changing the nodal spacing in the major portion of the craze. Fig. 3a shows the coarse mesh for the outer portion and Fig. 3b shows the fine mesh which includes the craze and the crack tip zone.

In order to estimate craze surface stresses it is necessary to know the applied load and the craze displacements. The total displacement, $2w$, of the two craze surfaces is given by

$$2w = 2v - \tau_0 \tag{4}$$

but $\tau_0 = 2v/\Lambda_c$ so that

$$2w = 2v(\Lambda_c - 1)/\Lambda_c \tag{5}$$

The displacement $w(x)$ of one craze surface is prescribed in the finite element input and the required stresses are included in the output. The most accurate estimates of stresses are at integration points, and stresses are plotted along a line joining the integration

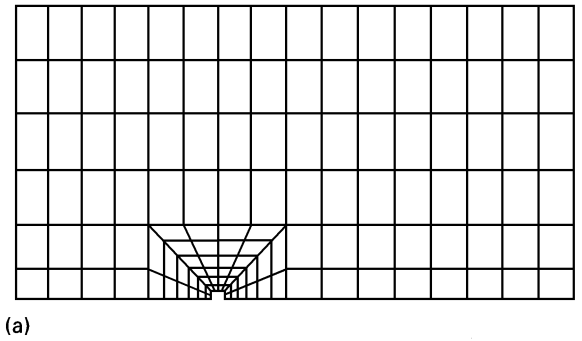

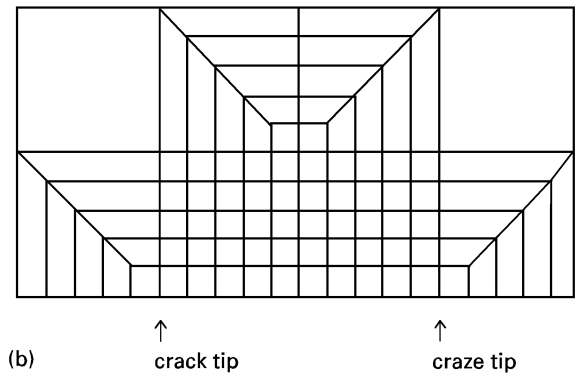

Figure 3 Finite element idealization of the compact tension (CT) specimen with (a) coarse mesh for the main part of sample and (b) fine mesh for the craze and crack tip region (crack and craze tips are indicated by arrows).

points nearest the craze. This line is parallel to the craze for the regular craze mesh shown.

3. Effect and evaluation of modulus

3.1. Effect on stress distribution

The craze stress distribution in a loaded sample depends on the applied load, the craze surface displacements and the elastic modulus E of the bulk polymer. The resultant stresses are usually determined, but it is possible to separate the effects of load and surface displacements as is illustrated schematically. The stress distribution of Fig. 4a is due to the applied load and is in fact a crack stress distribution, over the craze length, since the craze displacements are suppressed. The arrow indicates the position of the craze tip, and the origin of the graph (and subsequent ones) is an integration point 1.13% of the craze length ahead of the crack tip. This stress distribution is independent of the elastic modulus. The second stress distribution, Fig. 4b, is that of what is termed the self-surface stress. This is the distribution which would be required to maintain the craze surface displacements in the absence of the applied load [6]. The self-surface stress distribution is directly proportional to the elastic modulus of the polymer.

The stress distribution, computed including the load and the craze displacements, shown in Fig. 4c is the sum of the first and second stress profiles. The craze surface stress distribution is clearly very dependent on the material's modulus, and it will be shown

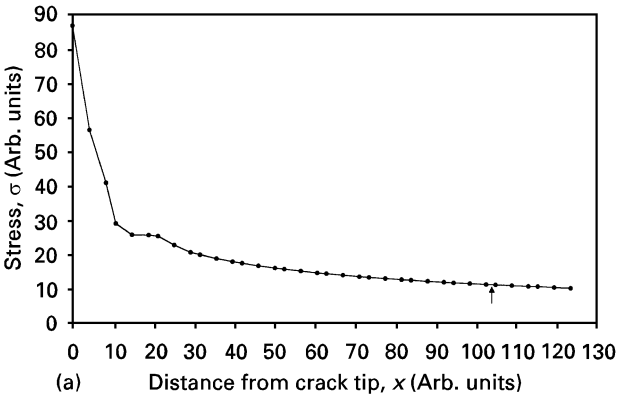

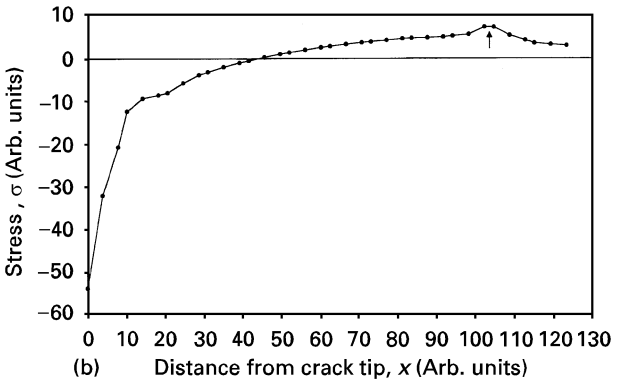

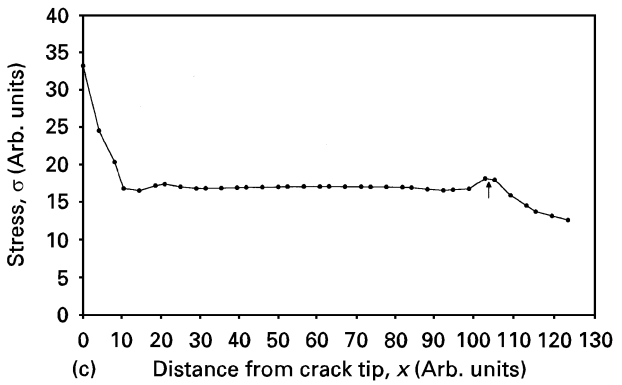

Figure 4 Stress distributions along a crack tip craze due to (a) load, and (b) craze surface displacements, and (c) the combined effects of load and craze displacements.

that there is a wide variation in the computed stress distributions, depending on the assumptions concerning E and its determination for a given case.

Stresses in crack tip crazes may also be estimated using the distributed dislocation stress analysis of Wang and Kramer [7]. The elastic modulus dependence is even greater in this case since the entire stress distribution is directly proportional to E.

3.2. Modulus evaluation

3.2.1. Fitting of the Dugdale model to the craze profile

Craze zones in polymers have the shape of thin wedges. A good description of the shape and size of this yielded zone at the crack tip can be provided by the plastic zone size model proposed by Dugdale [8]

and also by the cohesive force model of Barenblatt [9] which have been further developed by various authors (see reference [4]).

The Dugdale model implies a condition that there should be no singularity at the tip of the crack assuming a constant stress along the plastic zone at the crack tip. The relations of the dimensions of a Dugdale type craze zone to material parameters such as craze stress σ_c and elastic modulus E are described by equations containing the fracture mechanics parameter stress intensity factor K_I. The craze length s can be expressed by;

$$s = \frac{\pi}{8}\frac{K_I^2}{\sigma_c^2} \tag{6}$$

and the craze width $2v(x)$ at a distance x from crack tip is derived as;

$$2v(x) = \frac{8\,\sigma_c\, s}{\pi E^*}\left\{\xi - \frac{x}{2s}\ln\left(\frac{1+\xi}{1-\xi}\right)\right\} \tag{7}$$

with $\xi = (1 - x/s)^{1/2}, x > 0,$ and the crack tip at $x = 0$.

For the case of the maximum craze width at the crack tip $2v$ Equation 7 may be reduced to;

$$2v = \frac{K_I^2}{\sigma_c E^*} \tag{8}$$

To apply the Dugdale model to an interferometrically measured craze contour the following points should be remembered. As already noted in Section 2.1, the location of the craze tip and hence the craze length s cannot be measured directly, but can, in a similar way to the maximum craze width $2v$, only be obtained by extrapolation. Using the Dugdale model for extrapolation, the information contained in all measured points along the craze contour is fully utilized. In such a procedure, all the experimental points for a particular craze are used together with Equations 6 and 7 to calculate by iteration that value of s (and hence the corresponding values of E and σ_c) which minimizes the variation in E along the length of the craze.

The thus extrapolated position of a craze tip is shown in Fig. 2 as the closed circle (●). Also shown are the lines corresponding to the displacements $2v(x)$ calculated from Equation 7 using the fitted values of s, E and σ_c. Comparing the calculated and the measured values, a fairly good agreement along the contour of the loaded craze is observed while there is a major discrepancy in the case of the unloaded craze. This becomes reasonable taking into account that the Dugdale model is valid only if craze dimensions as well as the acting load and hence K_I – which causes craze formation – are consistent. Thus the Dugdale fit is only meaningful for a fully loaded craze.

In some cases, other loading conditions or different thermoplastics, the craze contour obtained by a Dugdale fit can differ to a greater extent from the measured data. This would result in an unrealistic craze length (and also maximum craze width). In such cases s and $2v$ obtained by mathematical (e.g., linear) extrapolations seem to be more reasonable. Such deviations of the craze shape from the contour

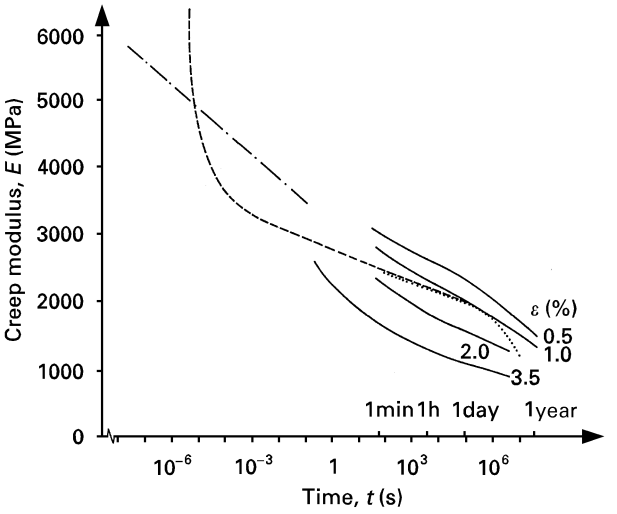

Figure 5 Creep moduli E in PMMA for different strains as a function of loading time t, determined from the crack tip region according to the Dugdale model, and from macroscopic measurements [4]. Key; (– - –) dynamic tests, (—) creep moduli (tensile tests), (- - -) creep moduli from Dugdale model for a moving crack and (… …) creep moduli from Dugdale model for a static crack.

predicted by the Dugdale model indicate other than constant stresses along the craze contour.

Fitting the Dugdale model to crack tip crazes measured under different loading conditions, such as crack propagation under quasi-static load, or craze growth under static load enables the determination of the rate dependent modulus E as a function of crack speed da/dt or loading time t. This was performed for PMMA over a wide range of crack speeds and times. The results are assembled in Fig. 5 as $E(t)$ over a time interval of almost 14 decades [4]. Comparing the moduli from the Dugdale fit with macroscopically measured creep moduli at different strains, the micromechanically determined data correspond at the onset of slow crack propagation (corresponding time of about 10^4–10^5 s) to a curve at about 1% strain, shifting towards higher strains during creep and with decreasing time turning back to lower strains in the transition regime to fast crack growth (about 10^{-4} s).

An elastic strain of about 1% just in front of a slowly propagating craze was determined using the fracture mechanics approach [4]. Increasing strains during creep and crack propagation due to local heating at an increasing crack speed seem to be most reasonable as well as decreasing strains at high rates due to a drop in molecular mobility. Thus the elastic modulus E determined by fitting the Dugdale model to the measured craze data can be assumed to be the modulus effective in the close vicinity of the crack tip craze under the given conditions.

3.2.2. Craze displacement method

This is similar to the previous method except that it is based on the displacement profile and not the thickness profile. This method will give higher estimates of E, which is inversely proportional to the displacement, and as can be seen from Equation 5 the ratio of the two estimates will be $\Lambda_c/(\Lambda_c - 1)$. Thus if Λ_c is 3 the

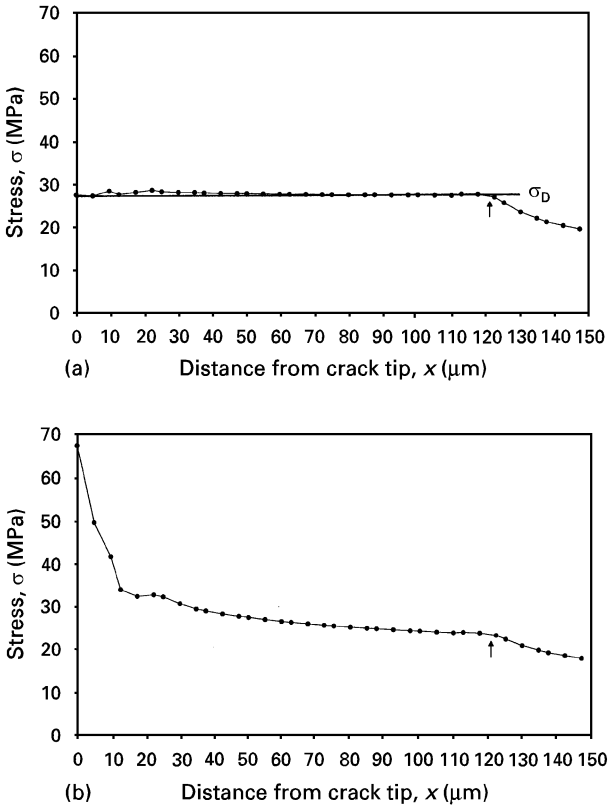

Figure 6 Craze surface stress distributions of a crack-tip craze in PMMA, loaded under creep conditions for 1.6×10^7 s at $K_I = 0.51$ MPa $m^{1/2}$, computed with Young's moduli of (a) 2.516 GPa (the Dugdale craze stress $\sigma_D = 27.25$ MPa is also indicated) and (b) 1.569 GPa.

modulus estimated by the displacement method is 50% higher than the Dugdale value. The former estimate is an unrealistically high one for the craze area and also it is unlikely to give a reliable estimate for the remainder of the sample since it is based on measurements at the craze interface. However, the craze displacement method is of interest since it should be the modulus that produces the constant stress distribution predicted by the Dugdale model. This is checked by the finite element method.

Idealized displacements (contour fitted to the Dugdale model) are used although the analysis is based on a long-term, *ca.* 6 months, creep craze in PMMA which had an almost constant extension ratio and a craze thickness profile in close agreement with the model. The moduli used in the computation are those estimated for the actual craze, i.e. 2.516 GPa from the displacement method and 1.569 GPa from the thickness profile. Fig. 6(a and b) display the two stress distributions due to the two separate moduli. The one with the greater modulus is in very close agreement with the Dugdale stress, which is also shown, while the lower modulus gives a distribution which, as expected, is consistent with previous results [1–3] since the same method was used to evaluate E. It should be pointed out that there is usually some additional inaccuracy in the finite element results for the element adjacent to the crack tip. This was in fact the case when initially, the prescribed craze displacement at the crack tip was set equal to the theoretical value. The computed stress at the Gauss point nearest

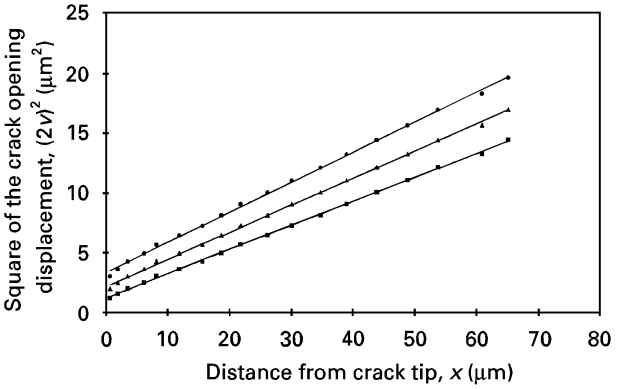

Figure 7 Variation of the square of the crack opening displacement (in a PMMA specimen loaded for 8.5×10^4 s at $K_I = 0.51$ MPa $m^{1/2}$) with distance from crack tip for initial fringe order, n_0, values of; (■) 3, (▲) 4 and (●) 5.

the tip was 6.7 MPa below the Dugdale stress while the stresses at the other two points were about 2 MPa too high. The prescribed displacement solely at the crack tip node was reduced by 2.7% in order to obtain the shown stress distributions.

3.2.3. Crack surface displacement method

Displacements of the crack surface are calculated from the interference optics measurements. The reduced modulus E^* may be calculated from the equation

$$2v(r) = \frac{8K_I}{E^*}\left(\frac{r}{2\pi}\right)^{1/2} \tag{9}$$

where K_I is the stress intensity factor in Mode I, r is a polar co-ordinate with the origin at the crack tip and $E^* = E$ in plane stress or $E^* = E/(1 - \nu^2)$ in plane strain, respectively.

It can be seen from Equation (9) that E^* may be calculated from the slope of a graph of $(2v)^2$ against r. It is seen from Fig. 7 that there is an excellent correlation (the correlation coefficient ranging from 0.99949 to 0.99971) for the three shown cases. The exact fringe order is not known and the three lines correspond to three possible initial fringe orders n_0, which must be added to the fringe order along the crack. Due to the presence of the craze, the crack tip displacement is non zero and hence the straight lines do not pass through the origin. The method has potential but some modification is necessary. There is uncertainty about the initial fringe order and in fact if different fringe orders from those in the figure are assumed $(2v)^2$ and r are still highly correlated with the correlation coefficients being slightly less than those quoted in which n_0 ranges from 3 to 5. It is also desirable to apply a correction to allow for the effect, on the crack, of the craze displacements and this is performed in the next section.

3.2.4. Crack displacements with finite element analysis

This method is based on a combination of interference optical measurements and finite element

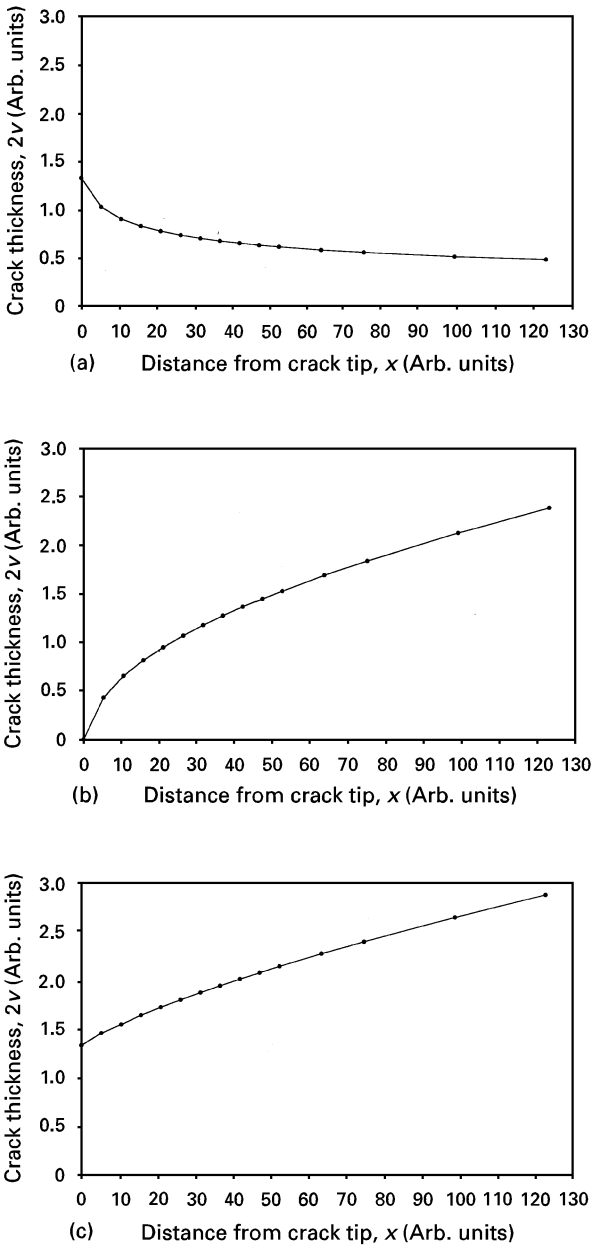

Figure 8 Displacements of one crack surface due to (a) prescribed craze displacements, and (b) load, and (c) the combination of load and craze displacements.

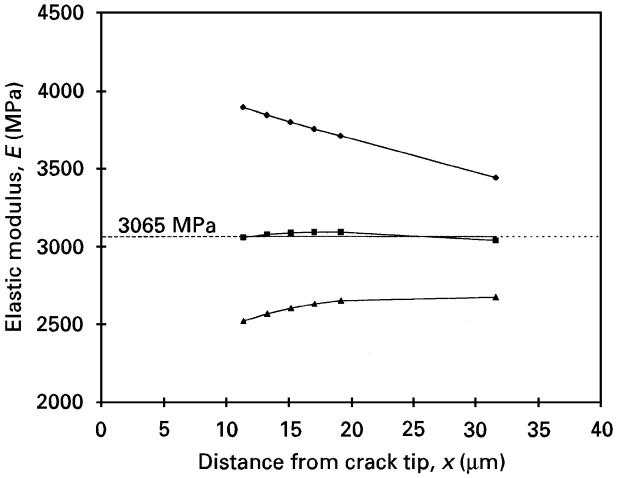

Figure 9 Estimated modulus values against distance from crack tip for initial fringe orders of; (◆) 3, (■) 4 and (▲) 5 (same specimen as Fig. 7).

computations of the crack displacements. The latter procedure is discussed first and is schematically illustrated in Fig. 8(a–c). The resultant displacement is usually determined but it is more efficient to separate the effects of the load and the prescribed displacements. These effects differ from those of the stress since the displacements due to the load are affected by the modulus whereas those due to the prescribed displacements are not. Crack displacements due to the latter are shown in Fig. 8a. Since the prescribed craze displacements are set to zero when computing the displacements due to the load, the origin of the calculated displacements will be the true crack tip. These displacements are calculated using an E-modulus which may be selected arbitrarily. Crack displacements solely due to the load are shown in Fig. 8b whilst Fig. 8c shows the resultant displacement profile. The latter is compared with the measured profile and the E value used in the computation is varied until the measured and calculated profiles agree. This is essentially the method used to evaluate E although the actual procedure slightly differs as is described in the following paragraph.

An arbitrary initial fringe order is selected and the resultant displacement at selected points on one craze surface is estimated from the measured displacement profile. The chosen points correspond to nodal positions along the crack, if the nodes nearest the crack tip are ignored. Since the crack displacements due to the craze are independent of the modulus they can be calculated at this stage even though the modulus is unknown. These displacements are subtracted from the measured ones to give estimates of the true crack displacement v_t, i.e., the displacement due to the load alone. The corresponding finite element value, v_{fe}, of the latter is calculated using a modulus of 1 GPa. Since the modulus is inversely proportional to displacement, a Young's modulus can be easily calculated using;

$$E = \frac{v_{fe}}{v_t} \tag{10}$$

If the assumed fringe order is correct, then consistent values of E will be obtained at the nodal positions. If not, every value of v_{fe} is increased by one-quarter of the wavelength of the monochromatic light used, for every increase of 1 fringe in the new assumed initial fringe order. An example of these calculations, using the data of Fig. 7, is shown in Fig. 9 where the estimated modulus is plotted against distance from the crack tip. If the assumed initial fringe order at the crack tip is too low then the modulus will be overestimated whereas it will be underestimated if the fringe order is too high. In both cases the error decreases as the distance from the crack tip increases. It is seen that E is almost constant for an initial fringe order n_0 of 4. The estimated modulus is 3.065 GPa which is clearly significantly different from the Young's modulus of 1.789 GPa obtained from the craze profile. This method, based on displacements of the crack, which

carries no normal stress, is considered to give a good estimate of the modulus of the sample since the strain levels are low both in the region near the crack and in the major part of the remainder of the specimen. This estimate of E is in this case a first approximation since the crack displacements due to those of the craze are no longer independent of the modulus when the sample is not of constant modulus.

4. Craze surface stress computation

Computations are carried out with two different material moduli, one for the coarse mesh of Fig. 3a, and the other for the fine mesh region shown in Fig. 3b. Two cases are selected to illustrate the method. In the first case the fine mesh region has the lower modulus whereas it has the higher modulus in the second case.

4.1. Creep test

In this test, using PMMA the craze grew while the crack remained stationary. The example chosen is for a time of 84.7×10^3 s which is slightly less than one day. Clear fringe patterns are available for both the craze and the crack. The crack displacements were analysed in Sections 3.2.3 and 3.2.4, yielding a modulus of 3.065 GPa in the major part of the specimen. The stress distribution is calculated with this modulus in the coarse mesh and in the fine mesh the modulus obtained from the craze profile of 1.789 GPa. The resultant distribution is plotted in Fig. 10a with the distribution for a single modulus of 1.789 GPa shown for comparison in Fig. 10b. The latter is in fact the distribution which would have been predicted by the previous method [1–3]. The introduction of the second modulus in the region outside the craze area clearly has a very significant effect on the calculated stress distribution. Any possible crack tip singularity is cancelled which is consistent with the observation that the crack remains stationary as the craze grows. There appears to be a slight stress concentration at the craze tip. This is because the position of the craze tip has to be estimated by extrapolation of the interference fringe pattern in the tip region and, in this case, linear extrapolation appeared to be more realistic than fitting the Dugdale model in this particular region.

4.2. Crack propagation

The interference fringe pattern has been remeasured in PMMA for a craze at the tip of a crack propagating at a rate of 270 mm s^{-1}. It was not possible to measure the fringe pattern due to the crack opening during crack propagation. This may be because of the insufficient reflectivity of the freshly created crack planes before the broken fibrils have retracted. In the finite element analysis a modulus of 5.054 GPa, obtained from the craze thickness profile, was used for the fine mesh region. Since the crack displacements were not known, the manufacturers measured value [10] of 3.3 GPa was used for the modulus of the remainder of the specimen. The resultant stress distribution is plotted

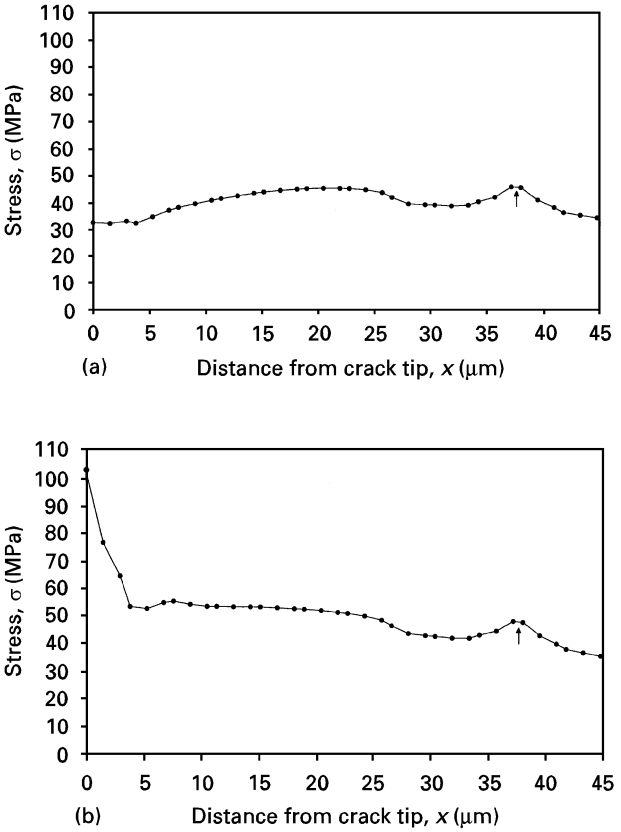

Figure 10 Craze surface stress distribution in a creep test ($K_I = 0.51$ MPa m$^{1/2}$, same specimen as Figs 7 and 9) determined using (a) different moduli in craze vicinity (1.789 GPa) and in the bulk (3.065 GPa) and (b) a single modulus (1.789 GPa).

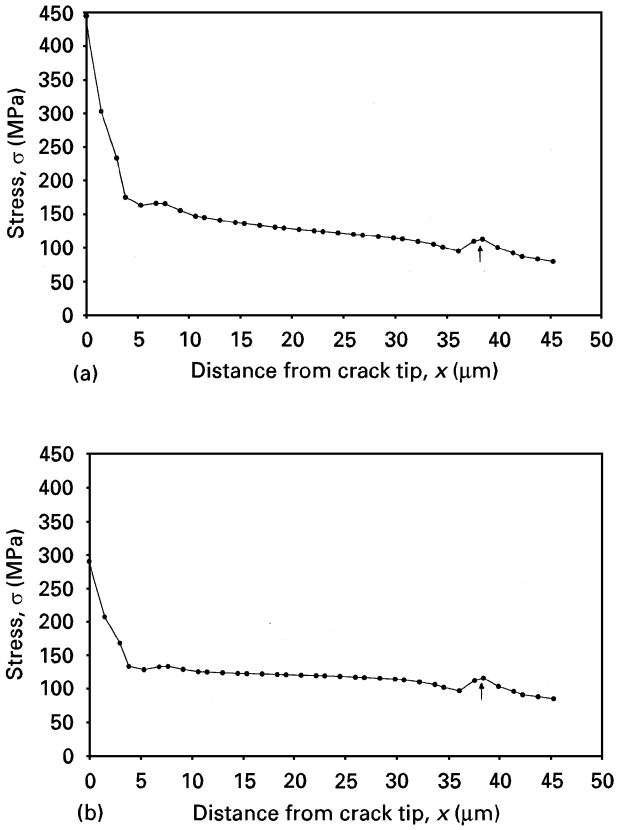

Figure 11 Craze surface stress distribution at the tip of a propagating crack in PMMA ($K_I = 1.25$ MPa m$^{1/2}$, $v = 270$ mm s^{-1}) determined using (a) different moduli in craze vicinity (5.054 GPa) and in the bulk (3.3 GPa) and (b) a single modulus (5.054 GPa).

in Fig. 11a and the distribution for a single modulus of 5.054 GPa is displayed in Fig. 11b. Comparison of the two profiles reveals that in both cases there is a stress peak at the crack tip, which is consistent with further crack propagation, but the stress is significantly higher with the bimodular analysis. Only the resultant stresses have been calculated and it should be pointed out that in the bimodular analysis the stresses solely due to the load are no longer independent of the modulus.

5. Conclusions

The calculated craze surface stress distributions are highly dependent on the modulus used in their evaluation. An analysis based on a constant modulus throughout the sample although it may be acceptable in short-term tests or if the applied strain is constant for most of the sample at a level which is not significantly different from that in the region immediately above the craze.

There are obviously more than two values of the Young's modulus at any time during these tests on compact tension specimens with crack tip crazes. Nevertheless, the area around the craze has a relatively high strain whilst the strain in the remainder of the specimen is low so that the two elastic moduli model is a good starting point and a reasonable approximation. The modulus in the zone near the craze is best obtained from the craze profile, using the method described in Section 3.2.1, and the crack displacement method of Section 3.2.4 should be used for the majority of the specimen.

Previously, similar stress distributions have been obtained for different loading systems whereas the new analysis provides distributions which are consistent with the tests as performed on PMMA. Thus, it is seen that the stress peak at the crack tip is suppressed in a case where the crack remains stationary and the craze continues to grow. In the case of crack growth, it is seen that at the crack tip the stress is increased and the crack will therefore continue to propagate through the craze. In many cases the difference in the two values of the modulus used in the analysis will be less than it is for the two discussed examples and the effect of the addition of the second modulus will be less dramatic. However, Figs 10(a and b) and 11(a and b) illustrate the potential of the new approach and also promise more realistic craze contour stresses for other thermoplastics.

Acknowledgements

We wish to thank the Deutsche Forschungsgemeinschaft (DFG), who funded the major part of this work, and the Sonderforschungsbereich (SFB 60) of the University of Freiburg for support for an additional visit (L. B.).

References

1. L. BEVAN, W. DÖLL and L. KÖNCZÖL, *J. Polym. Sci. Polym. Phys.* **B24** (1986) 2433.
2. *Idem.*, *Polym. Bull.* **16** (1986) 525.
3. L. KÖNCZÖL, W. DÖLL and L. BEVAN, *Colloid Polym. Sci.* **268** (1990) 814.
4. W. DÖLL and L. KÖNCZÖL, in "Advances in polymer science 91/92" edited by H. H. Kausch (Springer-Verlag, Berlin and Heidelberg, 1990) p. 137.
5. ADINA, A Finite Element Program for Automatic Dynamic Incremental Nonlinear Analysis, ADINA Eng. Inc. Watertown MA Dec. 1984.
6. B. D. LAUTERWASSER and E. J. KRAMER, *Phil. Mag.* **A39** (1979) 469.
7. W. V. WANG and E. J. KRAMER, *J. Mater. Sci.* **17** (1982) 2013.
8. D. S. DUGDALE, *J. Mech. Phys. Solids* **8** (1960) 100.
9. G. I. BARENBLATT, *Adv. Appl. Mechs.* **7** (1962) 55.
10. Röhm GmbH Chemische Fabrik, ® Plexiglas 233, Materialverhalten, Darmstadt 1971

Received 4 September 1995
and accepted 8 October 1996